

**Local order in aqueous solutions of rare gases and the role of the  
solute concentration: a computer simulation study with a  
polarizable potential.**

Paola Cristofori, Paola Gallo, and Mauro Rovere\*

*Dipartimento di Fisica, Università "Roma Tre",*

*INFN Roma Tre and Democritos National Simulation Center*

*Via della Vasca Navale 84, 00146 Roma, Italy.*

**Abstract**

Aqueous solutions of rare gases are studied by computer simulation employing a polarizable potential for both water and solutes. The use of a polarizable potential allows to study the systems from ambient to supercritical conditions for water. In particular the effects of increasing the concentration and the size of the apolar solutes are considered in an extended range of temperatures. By comparing the results at increasing temperature it appears clearly the change of behaviour from the tendency to demix at ambient conditions to a regime of complete solubility in the supercritical region. In this respect the role of the hydrogen bond network of water is evidenced.

PACS numbers: 61.20.Ja, 61.20.-p, 61.25.-f

## I. INTRODUCTION

The study of apolar aqueous solutions is of relevant interest for understanding basic effects connected to the properties of water as a solvent. In presence of an apolar solute reorganization of water solvent is observed around the hydrophobic solute molecules. The ordering of water causes a decrease of entropy in competition with the enthalpic term which favours the solvation. The apolar molecules of solute tend to aggregate to reduce the local order of the water molecules. The balance between the entropic and the enthalpic terms determines the hydrophobic hydration phenomena<sup>1,2,3</sup>. The hydrophobic effect plays an important role in chemistry, biology, chemical engineering. In this respect aqueous solutions of rare gases are considered both in experiments and in computer simulations as prototype models for studying the behaviour of mixtures of water with apolar solutes.

The structural arrangements of the solute close to the solvent and the changes in the structural properties of water due to the solvent are also related to the behaviour of solubility. For apolar solute the solubility is approximately one order of magnitude smaller than in other solvent like liquid hydrocarbons. As temperature goes up solubility decreases toward a minimum and then sharply increases<sup>4</sup>. At supercritical conditions water becomes a good solvent for rare gases. This behaviour has been interpreted in the computer simulation studies of Guillot and Guissani<sup>5</sup> as an interplay between the energetic term which favours the solubility of larger solutes and the entropic term which depresses the solubility at increasing size.

Only recently it has become possible to perform experimental studies of the structural correlations in aqueous solutions of non polar molecules with large neutron and synchrotron radiation facilities<sup>6,7,8,9</sup>. In particular neutron diffraction studies performed on dilute mixtures of rare gases in supercritical water<sup>9</sup> evidenced that the strong increase of the solubility with temperature could be related to the changes in the hydrogen bond network taking place in water approaching supercritical conditions.

A number of computer simulation studies have been performed since the pioneering work of Geiger, Rahman and Stillinger<sup>10</sup> on aqueous solutions<sup>5,11,12,13,14,15,16,17,18,19</sup>. Most model potentials introduced to reproduce the properties of liquid water by computer simulation are not able to predict the modification of the hydrogen bond network of water in the supercritical states evidenced by experimental results<sup>20</sup>. If polarizability is taken into account

there is a good improvement in the agreement with the experiments<sup>21</sup>.

Computer simulation of the temperature dependence of the structural properties of water and rare gases mixtures from ambient to supercritical conditions with the use of the polarizable potential BSV have been recently performed<sup>22</sup>. This potential was proposed for pure water by Ruocco and Sampoli<sup>23</sup> and later adapted by Brondholt, Sampoli and Vallauri<sup>24</sup> with a more refined fit of the potential parameters. The BSV potential is able to reproduce qualitatively the changes in the site-site correlation function of water<sup>21</sup> in the supercritical region. With the BSV potential at very low fixed concentration<sup>22</sup> a close agreement with the neutron diffraction experiments performed in the same supercritical conditions<sup>9</sup> is found.

We now consider the effects of increasing both concentration and size of the solute atoms at ambient and at supercritical conditions in a computer simulation of aqueous solutions with the BSV potential. We introduce as a further refinement of the model the polarizability of the solute atoms which is expected to play a non negligible role in the case of solutes of large size. We are motivated in this study by preliminary experiments that have been performed in supercritical water at increasing rare gas concentration<sup>25</sup>. In the structural studies of aqueous solutions the role of the concentration of the solute on the microscopic structure of the systems has been studied for different polar species with some controversial interpretation of the results<sup>12,14</sup>. In particular the question concerns how the increase of the solute concentration could improve the ordering of the solvent.

In the following we present results of MD simulations performed on solutions of argon and xenon. For the water-argon system experimental results at supercritical conditions will become available in a short time<sup>25</sup>. Simulation on xenon can help to clarify the effect of changing the size of the solute.

## II. COMPUTER SIMULATION WITH SOLUTE POLARIZABILITY

Mixtures of water and rare gases have been simulated by Molecular Dynamics (MD) in the microcanonical ensemble. The interaction of the water molecules is determined by the polarizable potential BSV<sup>23,24</sup>. This potential has the same geometry as the TIP4P<sup>26</sup> with a polarizable dipole moment placed on the center of mass of the molecule. The parameters are the two positive charges on the hydrogens, the Lennard-Jones potential parameters on the oxygen and the position of the negative charge displaced with respect to the oxygen.

The polarizability of water is introduced by an induced dipole  $p_i = \alpha E_i$  calculated from the local electric field  $E_i$  with an iterative procedure and by assuming an isotropic polarizability fixed to the value for water molecules<sup>23</sup>  $\alpha = 1.44 \text{ \AA}^3$ . In the following we use for water the parameters determined in ref.<sup>24</sup>. The parameters of the Lennard-Jones potential and the polarizability constants  $\alpha$  for the rare gases used in the present simulations are  $\epsilon/k_B = 125.0 \text{ K}$ ,  $\sigma = 3.415 \text{ \AA}$ ,  $\alpha = 1.586 \text{ \AA}^3$  for *Ar* and  $\epsilon/k_B = 232.0 \text{ K}$ ,  $\sigma = 3.980 \text{ \AA}$ ,  $\alpha = 4.0 \text{ \AA}^3$  for *Xe*. The usual Lorentz-Berthelot mixing rules have been employed.

The simulations have been carried out with the minimum image convention and a cut-off of the interactions at half of the box length. The reaction field has been used to take into account the long range part of the electrostatic interactions. The thermodynamical points explored range from ambient to supercritical conditions. In the simulations presented here a total number of 256 particles is simulated with the number of water molecules which varies depending on the concentration of the solute. The volume of the box is adjusted to obtain the chosen density. In the following we will present results obtained at ambient conditions and at the supercritical temperature  $T = 673 \text{ K}$  and density  $\rho = 0.331 \text{ g/cm}^3$ . The solute concentrations investigated are  $x = 1 : 40$ ,  $1 : 30$ ,  $1 : 20$  and  $1 : 15$ .

### III. STRUCTURE OF THE AQUEOUS SOLUTIONS

#### A. Structure at room temperature

Our results on the site correlation functions of the water-argon system indicate that the increase of the concentration of argon has little effect at room temperature on the structure of water.

The effect appears more relevant when we consider xenon. The oxygen-oxygen site correlation functions for both cases are shown in Fig. 1 for the highest studied concentration of solute 1:15 and for pure water. While with Ar only an increase of the height and a slight modification of the first peak is observed, for increasing fraction of Xe the second and also the third shells of neighbors are enhanced, as clearly seen in the figure. In the inset of the figure we report the coordination number of the first shell. It changes from  $n_{OO} = 3.95$  at concentration 1 : 40 of argon to  $n_{OO} = 4.45$  at concentration  $x_{ar} = 1 : 15$ . The change is more relevant when we consider xenon for which we get  $n_{OO} = 4.55$  at  $x_{xe} = 1 : 40$  and

$n_{OO} = 5.21$  for concentration of  $x_{xe} = 1 : 15$ .

The changes in the oxygen-oxygen first peak height could be interpreted from two different points of view. It can be related to an enhancement of the water ordering at increasing solute concentration but it can also be considered as an effect of an enlargement of the local density of water<sup>12</sup>. While the average density of solvent decreases at increasing number of solute atoms, the fraction of solvent involved in the coordination shells decreases more slowly than the average. We shall comment below on this by comparing these results with those obtained in the supercritical region.

The loss of ordering in the water-solute correlation as the rare gas concentration increases is evident from the changes in the arrangement of the solute atoms around the water molecules. The presence of a well defined peak in the solute-solute pair correlation functions, shown in Fig. 2 for the case of argon, indicates that the solute atoms are preferentially close each other. The first peak increases at increasing concentration while the first peak of the solute-oxygen and the solute-hydrogen pair correlation functions decreases at increasing concentration as shown in Fig. 3-4. In Fig. 2 we also observe for the higher concentration a slight shift of the first peak with a shortening of the minimum approach distance, a more marked shift is observed for the second shell.

At the lowest concentration explored ( $x_{ar} = 1 : 40$ ) the peak position of both the  $g_{OAr}(r)$  and the  $g_{HAr}(r)$  are located approximately at 3.5 Å according to the idea that the solute is interstitial in the hydrogen bond network of the solvent and it is equidistant between oxygens and hydrogens.

By increasing the argon concentration the first peak of the  $g_{OAr}(r)$  goes down indicating that the solute atoms tend to stay more away from water as there are more of them in the system. An estimate of the corresponding first shell coordination numbers indicates that the number of oxygens close to an argon atom ranges from 19 to 16 upon increasing solute concentration from 1 : 40 to 1 : 15.

In the  $g_{HAr}(r)$  (Fig. 4) a shoulder is present around 4 Å due to the presence of hydrogens radially oriented with respect to the solute. In the  $g_{HAr}(r)$  the first peak merges with the shoulder and at concentration of 1 : 15 the first coordination shell of solute around hydrogens is not well defined anymore. These results clearly indicate the tendency to demix of the solutes. The hydrophobic effect becomes more marked when solute atoms are added and affects mainly the first shell of the solute around the water molecules.

With a solute of larger size like xenon the effect is even more enhanced at increasing concentration, as shown in Fig. 5-6. The height of the first peak of  $g_{OAr}(r)$  decreases dramatically with the xenon concentration. In the case of xenon the estimate of the first shell coordination numbers is less precise. We have however obtained a number of oxygens close to a xenon atom which ranges from 20 to 13 upon increasing solute concentration from 1 : 40 to 1 : 15. Consistently with what we found for the oxygen-oxygen coordination number (see inset of Fig. 1) the decrease of nearest neighbours around the solute is more marked for xenon. We observe finally that the first shell of xenon around hydrogens is already ill defined at the lowest concentration.

### B. Structure in the supercritical region

We consider now the high temperature region, which corresponds to the conditions of supercritical water ( $T = 673$  K and  $\rho = 0.331$  g/cm<sup>3</sup>).

For the lowest argon concentration investigated here the BSV model shows agreement with experiments performed with isotopic substitution<sup>22</sup>. The comparison with the experimental results is shown in the bottom panel of Fig. 7.

The change of solute concentration has little effect on the water-solute structure, at variance with the ambient conditions where the addition of solute atoms increases the tendency of the system to demix. In Fig. 7-8 we observe only a slight broadening of the oxygen-solute first peak at increasing concentration.

By comparing Fig. 8 with Fig. 5 we note that the increase of concentration at ambient conditions seems to have an effect on the oxygen-xenon structure similar to the effect of the temperature. However the interpretation is very different if we look to the water site correlation functions. In Fig. 9 the oxygen-oxygen structure at increasing solute concentration are compared at ambient and supercritical conditions. This comparison indicates that at ambient temperature the increase of the first peak of the  $g_{OO}(r)$  is at least partially due to an ordering effect induced by the solute concentration. In the supercritical region this effect is completely disappeared due to weakening of the tetrahedral local order of water.

In Fig. 10 are reported the  $g_{OO}(r)$  at supercritical conditions for mixtures of Ar and Xe at the concentration 1:15. They are compared with the pure water. The comparison with Fig. 1 show that the effect of increasing the size of the solute is much less evident that at

ambient conditions. Moreover the presence of the solute slightly reduces and shifts the peak, a tendency which is opposite to the one at ambient conditions.

#### IV. CONCLUSIONS

The use of a polarizable potential for water allowed a realistic study of the structural changes induced by the addition of an apolar solute to water from ambient up to supercritical conditions where non polarizable potentials are known to fail in reproducing water behaviour. As a further refinement a polarizable potential for the solute was also introduced in our simulation.

The increase of the solute concentration at ambient conditions causes a strong tendency to demix. The local order of water seems also to increase. These effects are more marked on increasing size of the solute.

It is evident that the tetrahedral network of water plays an important role in the demixing process since the weakening of the hydrogen bond network which takes place at supercritical conditions favours the solubility of the rare gases in water making almost negligible the effect of increasing the solute concentration and/or the size of the solutes.

Comparisons of our results with ongoing experimental studies on similar systems can help to shed light on the important phenomena related to the hydrophobic hydration.

---

\* Author to whom correspondence should be addressed: rovere@fis.uniroma3.it

<sup>1</sup> Eley D. D., 1939, *Trans. Faraday Soc.*, **35**, 1421.

<sup>2</sup> Frank H. S., and Evans M. W., 1945, *J. Chem. Phys.*, **13**, 507; Frank H. S. and Wen W. Y., 1957, *Discuss. Faraday Soc.*, **24**, 133.

<sup>3</sup> Ben-Naim A., 1989, *J. Chem. Phys.*, **90**, 7412.

<sup>4</sup> Fernandez-Prini R., and R. Crovetto R., 1989, *J. Phys. Chem. Ref. Data*, **18**, 1231.

<sup>5</sup> Guillot B., and Guissani Y., 1993, *J. Chem. Phys.*, **99**, 8075.

<sup>6</sup> Broadbent R. D., and Neilson G. W., 1994, *J. Chem. Phys.*, **100**, 7453.

<sup>7</sup> Filipponi A., Bowron D. T., Lobban C., and Finney J. L., 1997, *Phys. Rev. Lett.*, **79**, 1293.

<sup>8</sup> Bowron D. T., Filipponi A., Lobban C., and Finney J. L., 1998, *Chem. Phys. Lett.*, **293**, 33.

- <sup>9</sup> Botti A., Bruni F., Isopo A., Modesti G., Oliva C., Ricci M. A., Senesi R., and Soper A. K., 2003, *J. Chem. Phys.*, **118**, 235.
- <sup>10</sup> Geiger A., Rahman A., and Stillinger F. H., 1979, *J. Chem. Phys.*, **70**, 263.
- <sup>11</sup> Zichi D. A., and Rossky P. J., 1985, *J. Chem. Phys.*, **83**, 797.
- <sup>12</sup> Vaisman I. I., and Berkowitz M. L., 1992, *J. Am. Chem. Soc.*, **114**, 7889.
- <sup>13</sup> Forsman J., and Jönson B., 1994, *J. Chem. Phys.*, **101**, 5116.
- <sup>14</sup> Puhovski Y. P., and Rode B. M., 1995, *J. Phys. Chem.*, **99**, 1566.
- <sup>15</sup> Bridgeman C. H., Buckingham A. D., and Skipper N. T., 1996, *Chem. Phys. Lett.*, **253**, 209.
- <sup>16</sup> Young W. S., and Brooks III C. L., 1997, *J. Chem. Phys.*, **106**, 9265.
- <sup>17</sup> Lynden-Bell R. M., and Rasaiah J. C., 1997, *J. Chem. Phys.*, **107**, 1981.
- <sup>18</sup> Ghosh T., Garcia A. E., and Garde S., 2002, *J. Chem. Phys.*, **116**, 2480.
- <sup>19</sup> Paschek D., 2004, *J. Chem. Phys.*, **120**, 6674.
- <sup>20</sup> Soper A. K., Bruni F., and Ricci M. A., 1997, *J. Chem. Phys.*, **106**, 247.
- <sup>21</sup> Jedlovszky P., Brodholt J. P., Bruni F., Ricci M. A., Soper A. K., and Vallauri R., 1998, *J. Chem. Phys.*, **108**, 8528.
- <sup>22</sup> De Grandis V., Gallo P., and Rovere M., 2003, *J. Chem. Phys.*, **118**, 3646.
- <sup>23</sup> Ruocco G., and Sampoli M., 1994, *Mol. Phys.*, **82**, 875.
- <sup>24</sup> Brodholt J., Sampoli M., and Vallauri R., 1995, *Mol. Phys.*, **86**, 149.
- <sup>25</sup> Ricci M. A., *private communication*.
- <sup>26</sup> Jorgensen W. L., Chandrasekhar J., Madura J. D., Impey R. W., and Klein M. L., 1983, *J. Chem. Phys.*, **79**, 926.



## Figure captions

Fig. 1. Comparison of the oxygen-oxygen pair correlation functions at room temperature of pure water (continuous line) with aqueous solution of 1:15 Ar (dotted line) and 1:15 Xe (long dashed line). In the inset: coordination number of the first shell of oxygen-oxygen as function of the concentration  $x$  of argon (circles) and xenon (triangles).

Fig. 2. Argon-argon pair correlation functions at room temperature at concentration of Ar: 1 : 40 (continuous line) and 1 : 15 (long dashed line).

Fig. 3. Oxygen-argon pair correlation functions at room temperature at different concentrations of Ar: 1 : 40, 1 : 30, 1 : 20 and 1 : 15 from the bottom.

Fig. 4. Hydrogen-argon pair correlation functions at room temperature at different concentrations of Ar: 1 : 40, 1 : 30, 1 : 20 and 1 : 15 from the bottom.

Fig. 5. Oxygen-xenon pair correlation functions at room temperature at different concentration of Xe:  $x_{xe} = 1 : 40, 1 : 30, 1 : 20, 1 : 15$  from the bottom.

Fig. 6. Hydrogen-xenon pair correlation functions at room temperature at different concentration of Xe:  $x_{xe} = 1 : 40, 1 : 30, 1 : 20, 1 : 15$  from the bottom.

Fig. 7. Oxygen-argon pair correlation functions at  $T = 673$  K at different concentration of Ar: 1 : 40, 1 : 30, 1 : 20 and 1 : 15 from the bottom. The open circles are the experimental results<sup>9</sup>.

Fig. 8. Oxygen-xenon pair correlation functions at  $T = 673$  K at different concentration of Xe: 1 : 40, 1 : 30, 1 : 20 and 1 : 15 from the bottom.

Fig. 9. Oxygen-oxygen pair correlation functions at  $T = 300$  K on the left and at  $T = 673$  K on the right with different concentration of Xe: 1 : 40 (continuous line), 1 : 15 (long dashed line). For  $T = 673$  K the two curves are indistinguishable.

Fig. 10. Oxygen-oxygen pair correlation functions at  $T = 673$  K at concentration 1:15 Ar (open triangles) and Xe (open square) compared with pure water (bold line). In inset a blow up of the first peak is reported.

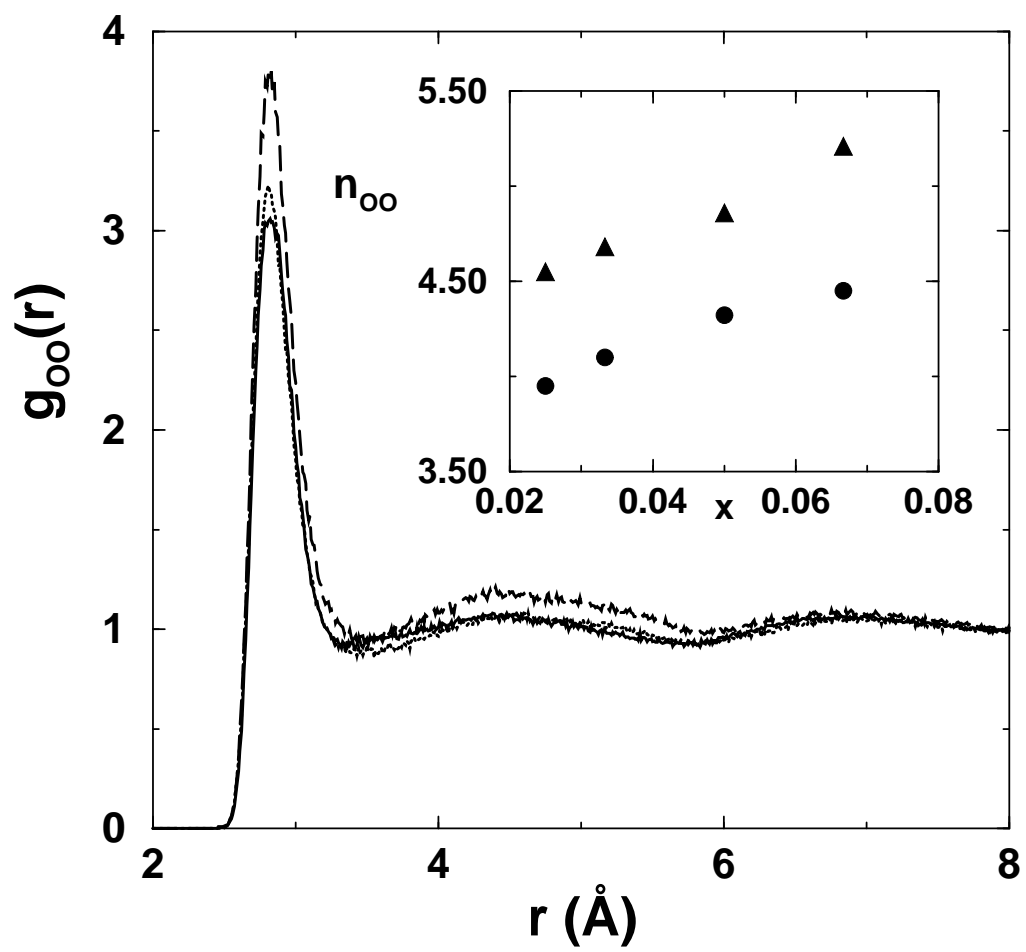


Figure 1 - P. Cristofori et Al.

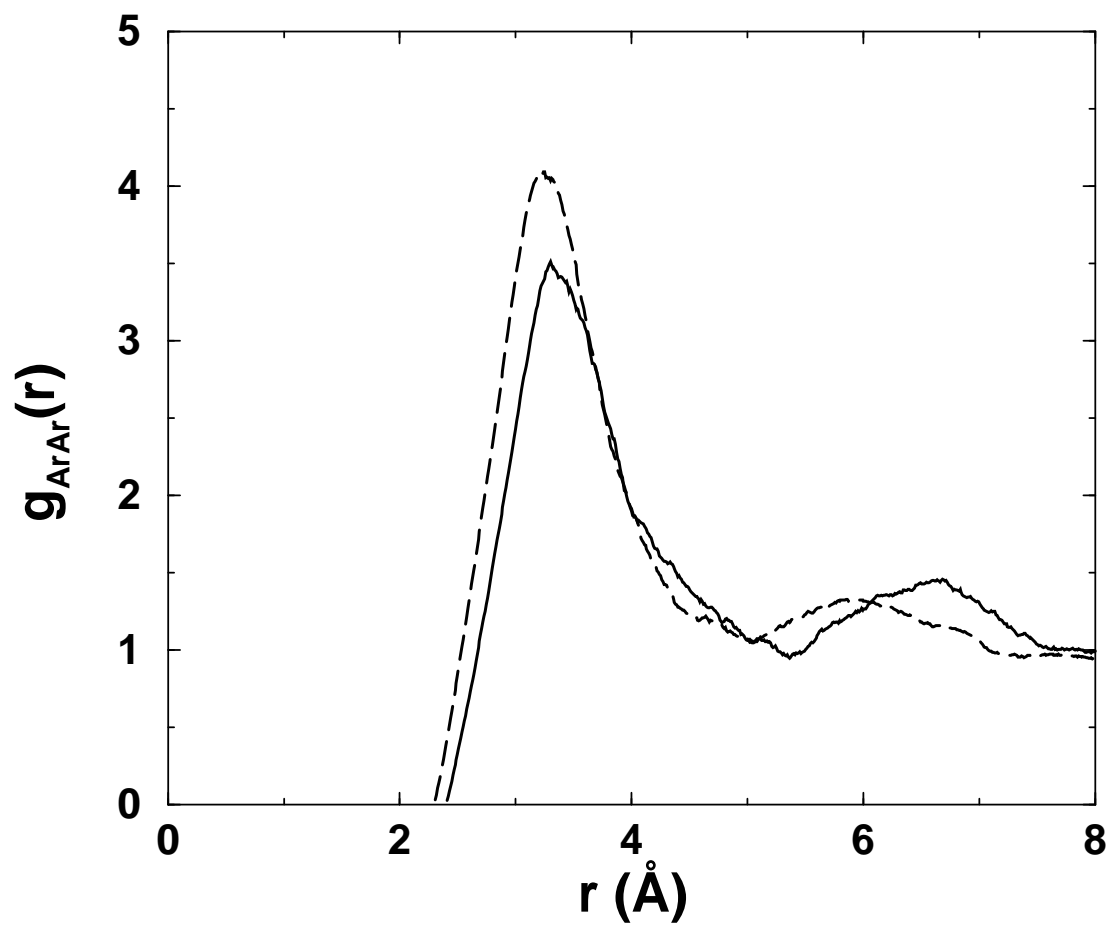


Figure 2 - P. Cristofori et Al.

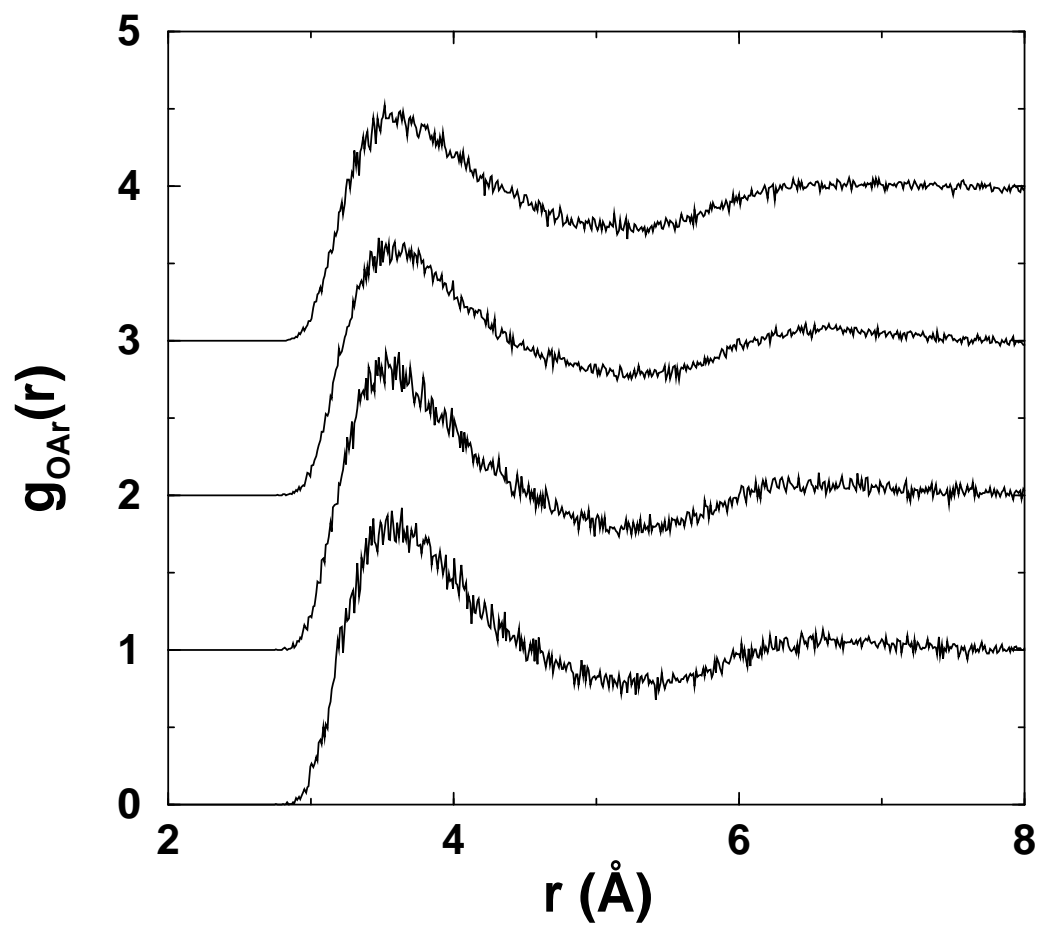


Figure 3 - P. Cristofori et Al.

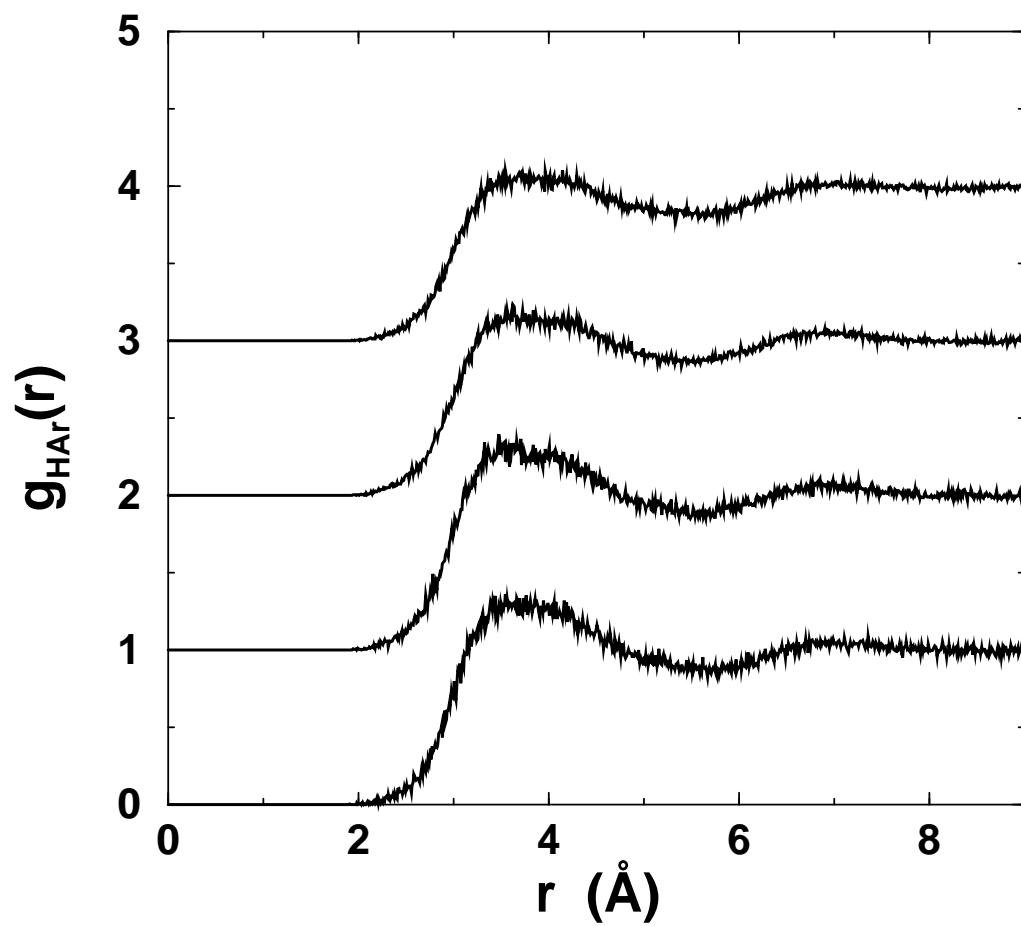


Figure 4 - P. Cristofori et Al.

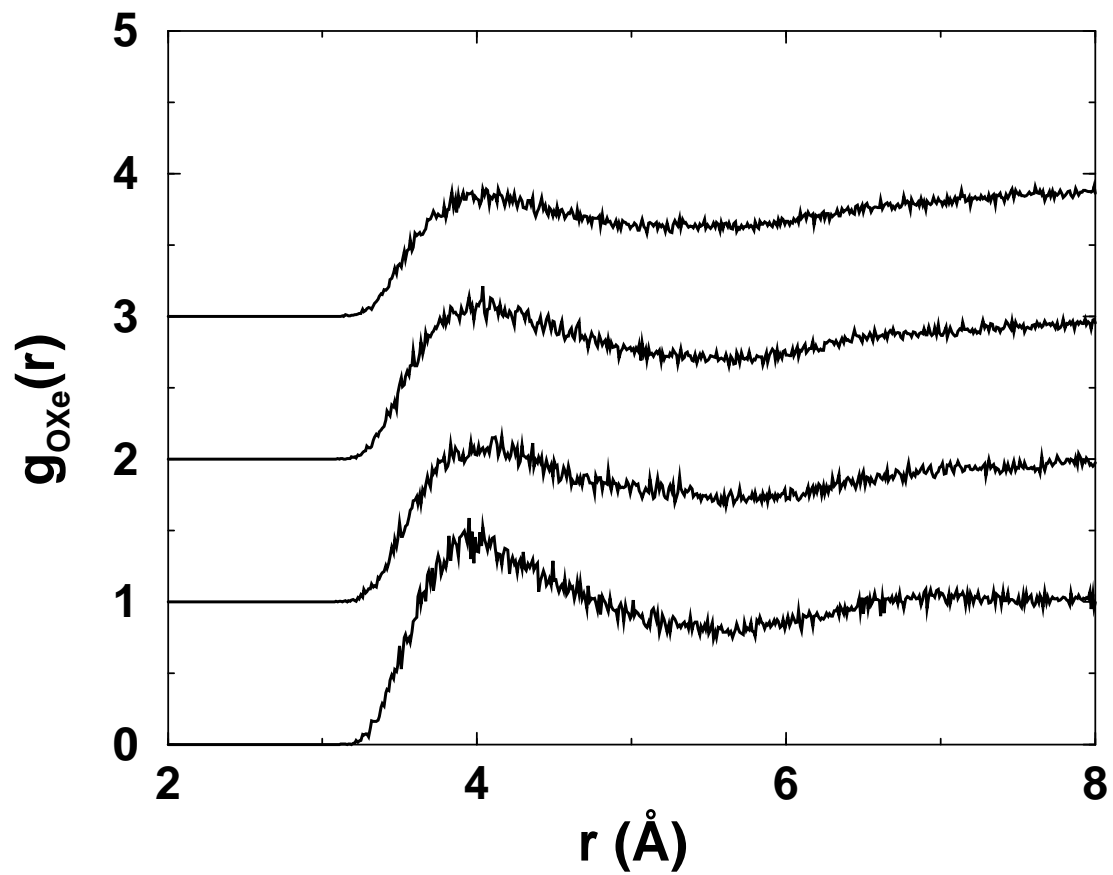


Figure 5 - P. Cristofori et Al.

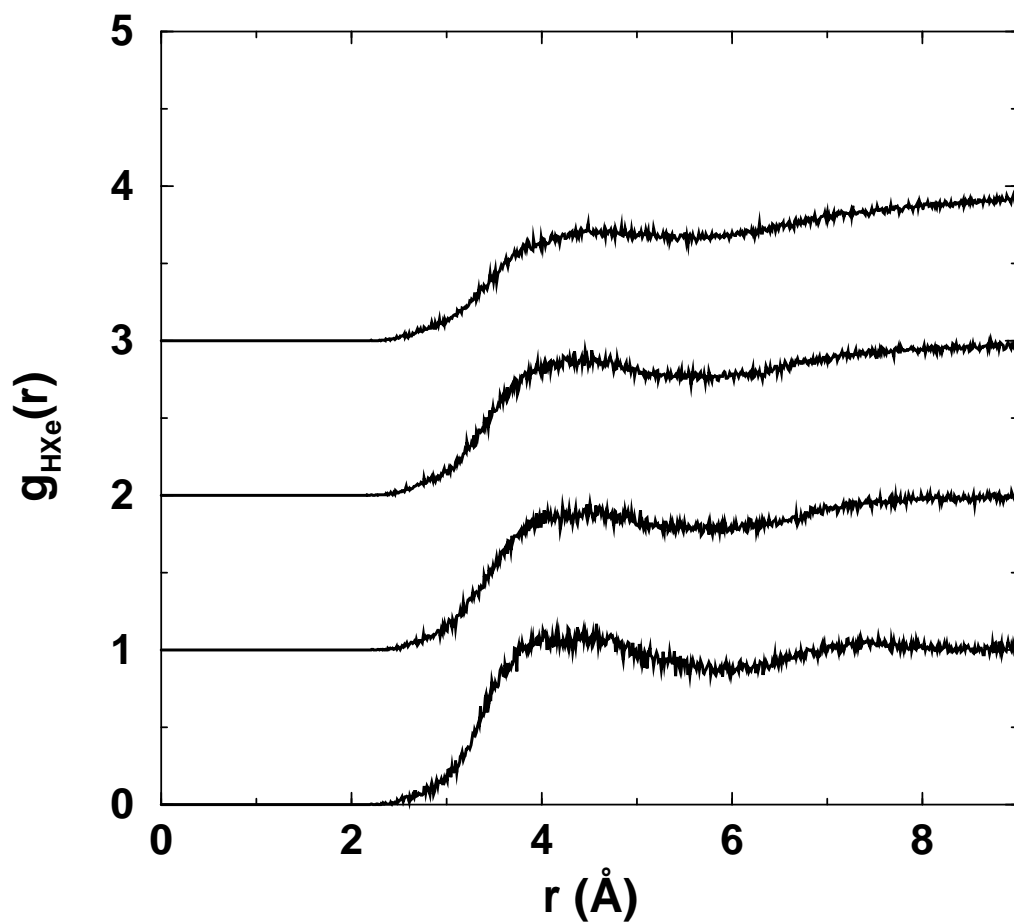


Figure 6 - P. Cristofori et Al.

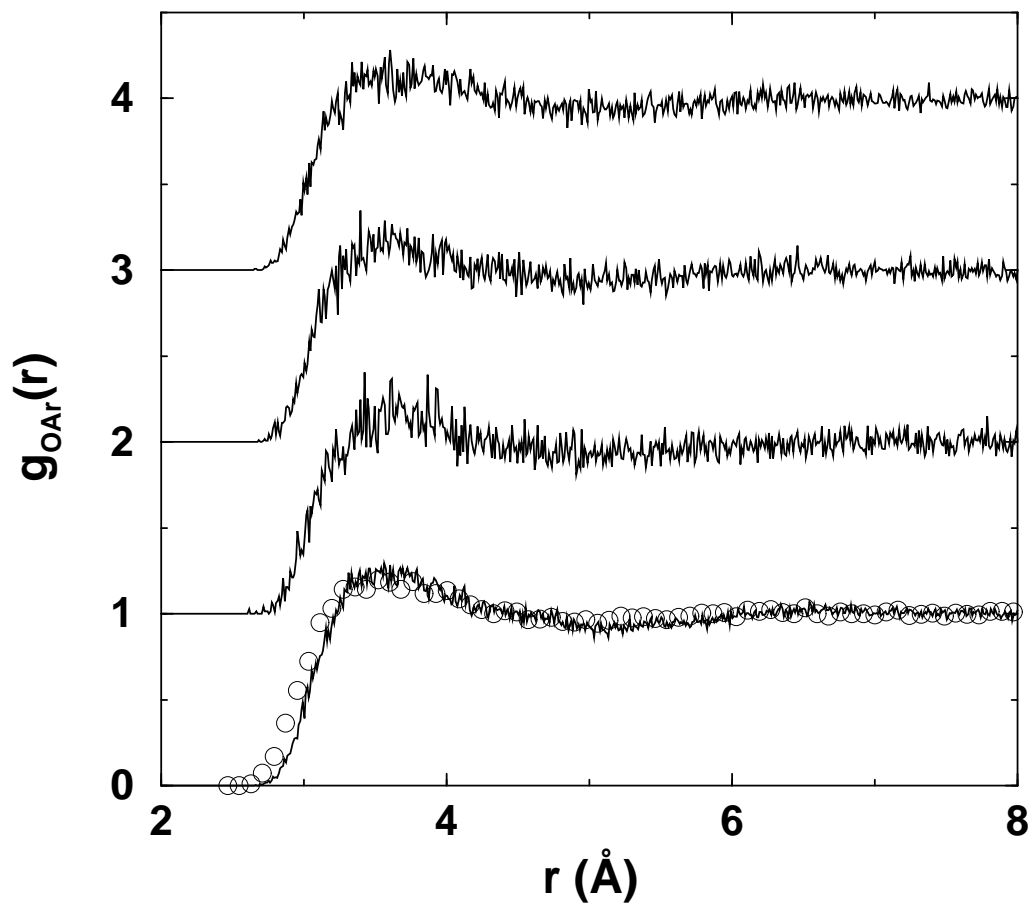


Figure 7 - P. Cristofori et Al.



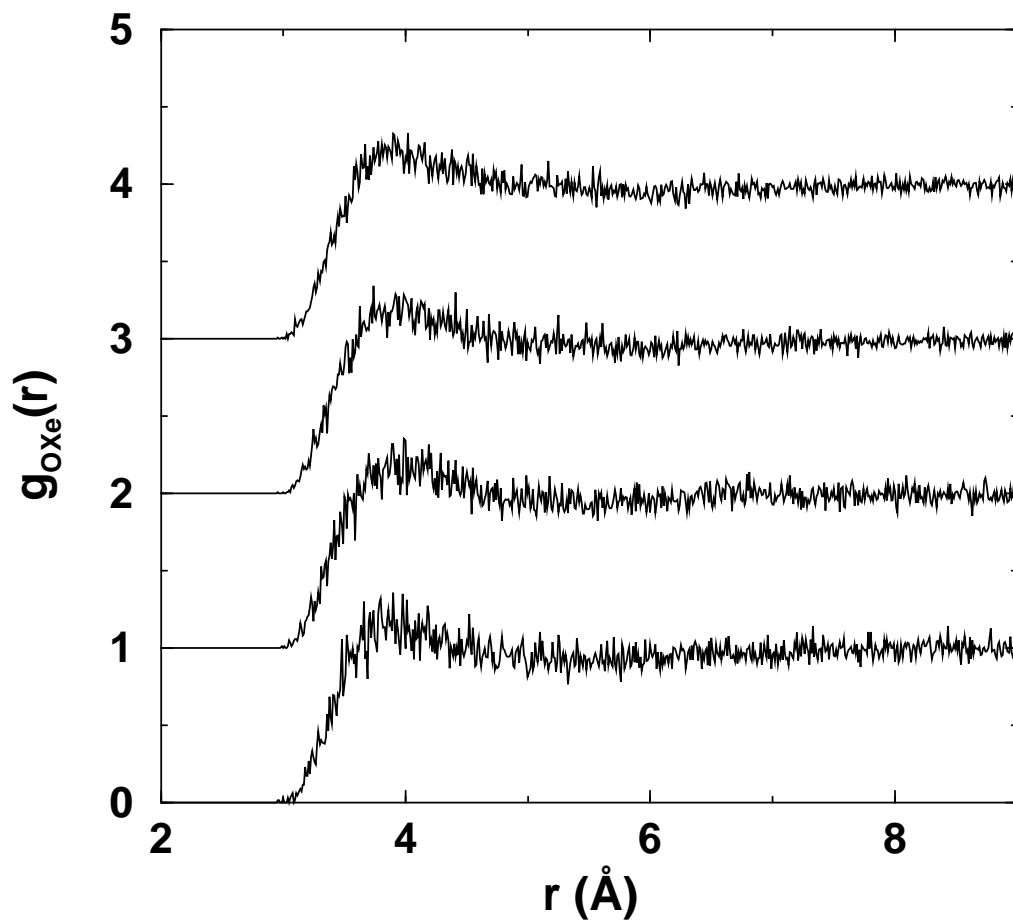


Figure 8 - P. Cristofori et Al.

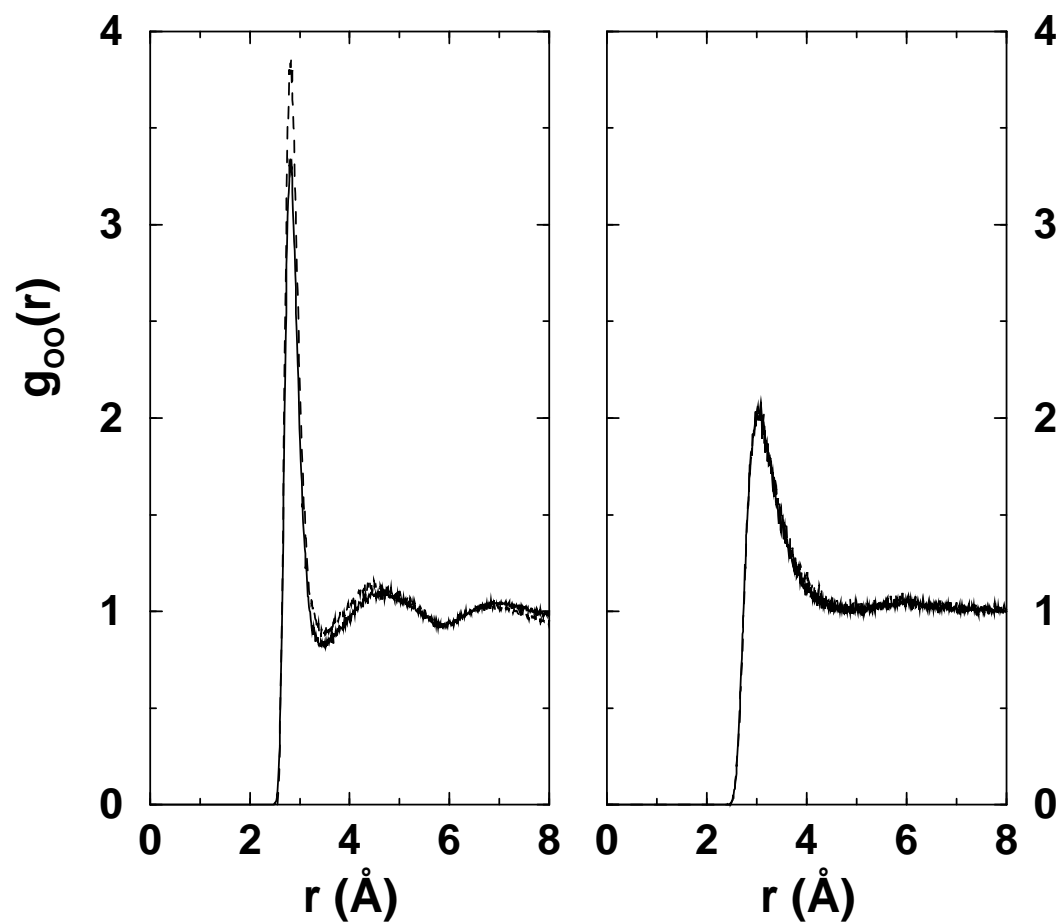


Figure 9 - P. Cristofori et Al.

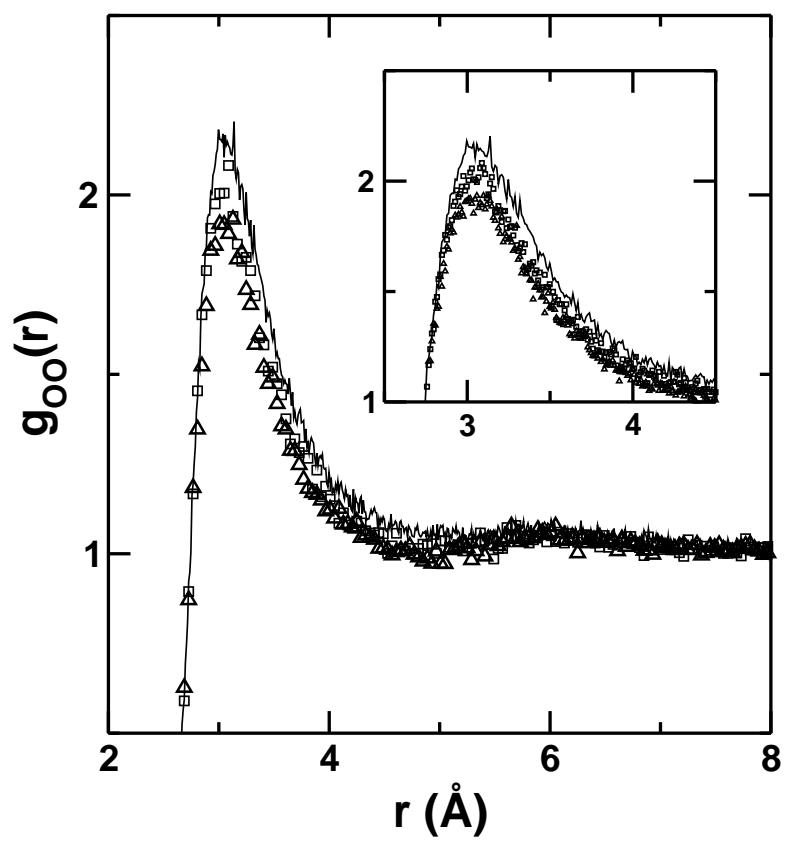


Figure 10 - P. Cristofori et Al.